



Cite this: *Analyst*, 2023, **148**, 5486

A layered cancer-on-a-chip system for anticancer drug screening and disease modeling

Magdalena Flont,^a Artur Dybko^b and Elżbieta Jastrzębska^{*a,b}

Recent advances in the development of microfluidic systems for the culture of complex and three-dimensional cell, tissue, and organ models allow their use in toxicity studies and mimicking many diseases. These types of *in vitro* models are important because of the huge advantages over standard two-dimensional cell cultures: better mimicking of *in vivo* conditions and more reliable response to the tested drugs. This report presents a new approach to modeling skin cancer (melanoma-on-a-chip) and breast cancer (breast cancer-on-a-chip) using the microfluidic systems. We designed a microfluidic device to co-culture cancer cells with non-malignant cells, which are the main component of the cancer micro-environment. In the construction of the microsystem, we used a scaffold in the form of a porous membrane made of poly(ethylene terephthalate), which enables the regular and reproducible arrangement of cells in the culture and maintains intercellular communication. To demonstrate the functionality of the microsystem, we used it to analyze the effectiveness of photodynamic therapy in the treatment of melanoma and chemotherapy in the treatment of breast cancer. The developed microsystem can be successfully used to model cancer diseases, especially with a layered arrangement of cells in the cancerous tissue, such as melanoma, ductal breast cancer, or breast cancer metastases to the skin.

Received 13th June 2023,
Accepted 11th September 2023

DOI: 10.1039/d3an00959a

rsc.li/analyst

Introduction

Miniaturization in biological and medical applications has been a leading trend over the last 20 years. Cell-on-a-chip systems are a common solution for improving laboratory research using cell cultures.¹ However, the development of complex and stable cellular systems that consider intercellular, inter-tissue or interorgan interactions remains a significant challenge in today's science. The current knowledge also lacks simple *in vitro* cell models that allow for advanced and reproducible imitation of disease states.²

Despite access to a vast base of cancer cell lines, the tissue model of the cancer structure is still difficult to achieve under *in vitro* conditions.³ Cancer is one of the leading causes of death in the world;⁴ therefore, there is a justified need to focus modern cell engineering on modelling cancer diseases in laboratory conditions. The development of a versatile system useful in modeling various types of cancer would significantly speed up the processes of testing drugs and anticancer therapies, and focus on personalized treatments. The difficulty in developing a universal tool for cancer modeling is the compli-

cated characteristics of this group of diseases: heterogeneous genotype and heterogeneity, as well as the role of the non-cancerous microenvironment, the presence of which is a factor limiting the development of cancer.^{3,5,6} Histopathological studies confirm that the complex cancer microenvironment contains numerous cancer cells surrounded by non-malignant components and co-embedded in a heterogeneous, vascularized and protein extracellular matrix (ECM). The cancer microenvironment includes a rich variety of immune cells, cancer-associated fibroblasts (CAFs), endothelial cells, pericytes, and other cell types.⁵ The cancer stroma is responsible for creating a specific ECM that fills the gaps between cells, enables them to contact and communicate with each other and affects their proliferation, playing a key role in the progression of cancer. Its components include glycosaminoglycans, proteoglycans, glycoproteins and numerous collagen fibers.⁷ Immune cells are also critical in the formation and development of cancer. Innate and adaptive immune cells can play both pro-cancer and anti-cancer roles in cancer biology. The immune response is often successful at initially eliminating the cancer cells. However, through a phenomenon known as immunoediting, cancer cells can acquire the ability to evade destruction by the immune system, leading to cancer progression.⁸

Many attempts have been made to mimic the very complex structure of a tumor with elements of its microenvironment under microfluidic conditions that mimic physiological flow conditions.⁹ So far, it has been confirmed that the most faith-

^aCenter for Advanced Materials and Technologies CEZAMAT, Warsaw University of Technology, Poleczki 19, 02-822 Warsaw, Poland.

E-mail: elzbieta.jastrzebska@pw.edu.pl; Tel: +48 22 234 7253

^bChair of Medical Biotechnology, Faculty of Chemistry, Warsaw University of Technology, Noakowskiego 3, 00-664 Warsaw, Poland



fully reflecting the structure of cancer under *in vitro* conditions are 3D models, such as spheroids, tumor organoids, hydrogel systems or cultures on scaffolds. Spheroids are the most popular 3D cancer models with many advantages for creating complex multicellular structures. The potential of spheroids to be used in preclinical studies on the cytotoxicity of anticancer drugs has been repeatedly confirmed.^{10,11} In recent years, self-assembling, three-dimensional cultures of cancer organoids derived from tumor biopsies have also become a promising alternative to conventional *in vitro* cultures. Cancer organoids can reflect the heterogeneous structure of the tumor and preserve gene mutations of a specific cancer type, giving a reliable response to drugs in cytotoxicity assays.¹²

However, there are cancers with a characteristic layered arrangement of cells in the tissue, including: skin cancer, ductal breast cancer, all epithelial cancers, colorectal cancer and respiratory diseases, including lung cancer. Despite the many advantages of popular 3D models such as spheroids or organoids, an alternative cellular model with a different arrangement of cells is still sought for layered types of cancer.

Malignant melanoma is a highly aggressive skin cancer originating from melanocytes. Although it accounts for only 4% of all skin cancers, the incidence of this type of cancer has tripled in recent decades.^{13,14} Melanoma is characterized by high mortality and significant metastatic potential. Treatment of this cancer type in the metastatic stage often does not bring satisfactory results, and melanoma cell invasion is a complex and poorly understood process. Research from recent years has confirmed that non-malignant skin cells, such as fibroblasts or keratinocytes, play a crucial role in melanoma development.¹⁵ It has also been confirmed that photodynamic therapy (PDT) may be used to treat early-stage melanoma.¹⁶ PDT is an anticancer therapy that uses a photosensitive drug (photosensitizer), a light source of appropriate power and wavelength, and oxygen dissolved in the tissue, the effect of which is the result of photocytotoxic reactions occurring in the tissues. Searching for a suitable photosensitizer is still challenging, showing high efficiency, active only under the influence of light, selectivity, and undergoing rapid metabolism.¹⁷ Ductal breast carcinoma (DCIS, ductal carcinoma *in situ*) is the most commonly diagnosed malignancy among women and is highly lethal in the metastatic stage.¹⁸ The crucial role of breast fibroblasts in the formation and development of this cancer has been proven,¹⁹ but there is still no standard treatment regimen. The basic procedure in treating breast cancer is reducing the diseased tissue and chemotherapy. It is worth noting that both cancers have a structure similar to layers, and metastatic breast cancers often give metastases to the skin (most often on the chest and abdomen), which in terms of phenotype resemble changes caused by melanoma.^{20,21}

The layered structure of the discussed types of cancer opens the perspective of reflecting the arrangement of cells involved in the formation and development of skin/breast cancer *in vitro* to best represent the disease *in vivo*. For this purpose, it is useful to use the cancer-on-a-chip approach, which gives the following:

(a) The possibility of reconstructing the complex cancerous microenvironment, of proven importance in the development of the disease, easy to monitor and control;

(b) The ability to overcome certain limitations of standard macroscale cultures that hinder rapid drug screening and disease modeling, *e.g.*, high consumption of reagents, cell culture only in two dimensions, lack of perfusion imitating blood movement, time-consuming analyses;

(c) The possibility of using additional structural elements such as scaffolds or porous membranes. Using such materials as a substrate for cells can reflect the three-dimensional arrangement of cells, change the availability of media and oxygen to cells, and study the penetration of drugs through layers of normal cells into cancer cells, as is the case in a physiological environment.

In addition, the layered cancer-on-a-chip model in studies of selected types of cancer with a layered arrangement of cells in the tissue may have a significant advantage over the spheroids or organoids. In contrast to organoids, the layered model is very versatile and can be widely used in drug screening.¹² In contrast to spheroids, the layered model does not only imitate the initial stage of a tumor, but is closer to a cancer tissue section. In addition, in this model, the arrangement of cells is not chaotic, but controlled. Thanks to this, the model allows not only to use it to study the cytotoxicity of compounds, but also to analyze the interactions between the components of the microenvironment and the cells that build the model, and even to study the migration and reorganization of cells under the influence of the studied factors. Spheroids are an ideal model for many cancer studies, but for some types of research they may have limitations, *e.g.* the presence of a necrotic core, which is not present in the layered model.²²

In the literature, there are several methods of obtaining layered culture, also in microfluidic systems, among which the use of porous membranes made of natural or synthetic materials is dominant. One of the materials is synthetic poly(ethylene terephthalate) which, due to its relative cheapness, ease of processing, non-toxicity and transparency, is widely used in organ-on-a-chip microsystems as a porous membrane. It has been used in microfluidic systems for layered culture of cells of various organs: intestine, heart, kidney, liver and cancer cells, *e.g.* cervical cancer.²³

In this report, we present a new approach to three-dimensional *in vitro* modelling of cancer using the cancer-on-a-chip system. We developed a new microfluidic system integrated with a porous poly(ethylene terephthalate) (PET) membrane as scaffold for layered co-culture of non-malignant and cancer cells. In contrast to other works,^{24,25} our cellular model imitates the structure of cancer because it is made of both: cancer cells and non-malignant cells as non-cancerous elements of the cancer microenvironment. The non-cancerous microenvironment elements are responsible for forming an extracellular matrix (ECM) and play a crucial role in carcinogenesis.²⁶ The layered arrangement of cells in the cell co-culture we proposed is analogous to the arrangement of cells of some solid tumors (including skin cancer, breast cancer, and breast cancer metas-



tases to the skin). Moreover, using a PET membrane may be an effective method of studying drug penetration into cancer cells through the layer of non-malignant cells.²⁷ The developed microsystem was used to study cyto- and photocytotoxicity of *meso*-tetraphenylporphyrin (TPP) (for skin co-culture) and cytotoxicity of doxorubicin (for breast co-culture). It was proved that the developed layered and heterogeneous cancer models could be used to study the penetration of drugs into cancer cells, interactions between cancer cells and non-malignant cells, and evaluate the effectiveness of anticancer drugs.

Materials and methods

Cell culture and chemicals

Four cell lines were used in the experiments. To develop a layered model of melanoma-on-a-chip a co-culture of human keratinocytes HaCaT obtained from ThermoFischer and malignant melanoma fibroblasts MeWo purchased from the American Type Culture Collection (ATCC) were used. Both cell lines were cultured in Dulbecco's modified Eagle's medium (DMEM, Biowest) supplemented with 10% vol. fetal bovine serum (FBS, Biowest), 1% vol. of streptomycin and penicillin solution (Biowest, the starting solution contained 10 000 units per mL of penicillin and 10 000 µg per mL of streptomycin) and 1% vol. L-Glutamine solution (Biowest, starting concentration = 200 mM).

To develop a model of ductal breast cancer-on-a-chip, a co-culture of primary cells – human mammary fibroblasts HMF, obtained from ScienCell Research Laboratories and breast cancer cell line MCF-7 from ATCC were used. The primary cells were cultured in Fibroblast Medium (ScienCell) supplemented with 2% vol. of fetal bovine serum (ScienCell), 1% vol. of streptomycin and penicillin solution (ScienCell, the starting solution contained 10 000 units per mL of penicillin and 10 000 µg per mL of streptomycin), and 1% vol. of L-glutamine solution (ScienCell, starting concentration = 200 mM). Breast cancer cells were cultured in Dulbecco's modified Eagle's medium (DMEM, Biowest) supplemented with 10% vol. of fetal bovine serum (FBS, Biowest), 1% vol. of streptomycin and penicillin solution (Biowest) and 1% vol. of L-glutamine solution (Biowest). Doxorubicin (DOX, Sigma) and *meso*-tetraphenylporphyrin (TPP, Sigma) were studied as chemical compounds used in anticancer therapies. DOX belongs to phase-specific anthracyclines and is a compound used clinically in the treatment of many types of cancer, including breast cancer.²⁸ TPP is a synthetic heterocyclic compound from the group of porphyrins and is clinically used in PDT to treat melanoma.²⁹

Design and fabrication of the microsystem

The microsystem was made of two poly(dimethylsiloxane) layers (PDMS, Sylgard 184, Dow Corning) and six porous poly(ethylene terephthalate) (PET) membranes. The PET membranes were put between the PDMS layers and sealed to them (Fig. 1). The PDMS layers (with external dimensions of 60 mm × 25 mm × 10 mm) had a symmetrical microstructure of six

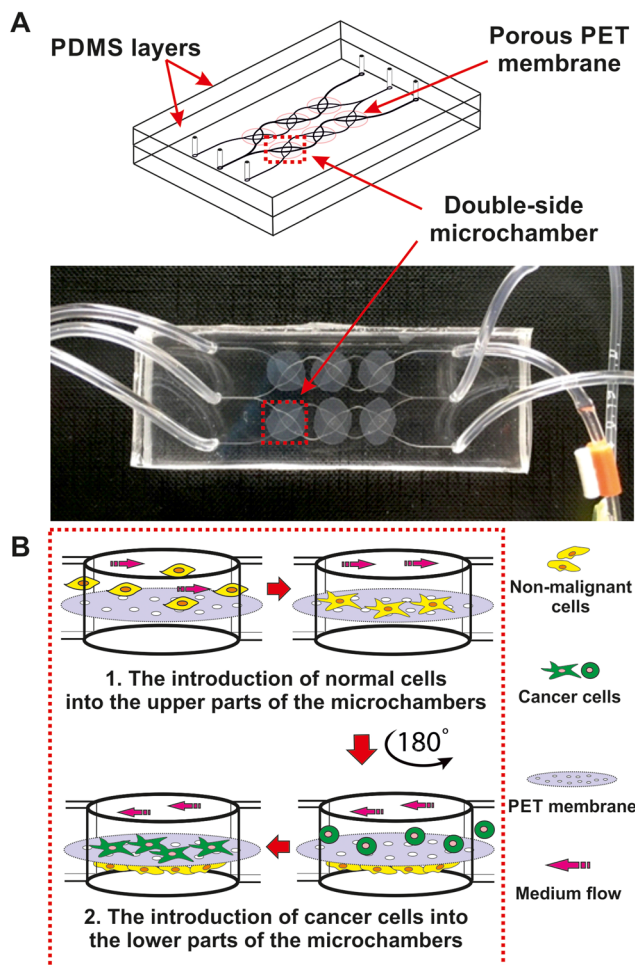


Fig. 1 (A) Geometry of the microsystem for 3D double-layered cell culture. (B) A scheme of seeding the cells on the PET membrane.

oval culture chambers arranged in two rows, connected by a network of rounded microchannels a diameter of 50 µm. The symmetrical microstructures of each PDMS layer were overlaid alternately, such that the culture chambers in the upper and lower PDMS layers did not wholly overlap but had a common culture section of approximately 2 mm × 2 mm. The common culture section was a two-sided chamber for layered cell co-culture (Fig. 1A). Inlet and outlet holes were made in the top PDMS layer. Thanks to them, it was possible to supply culture media and reagents separately in the upper and lower part of the culture chamber. Reagents and cell suspensions were introduced into the microsystem using peristaltic pumps (Ismatec Reglo ICC).

PET membranes, which contained pores with a diameter of 0.4 µm and a density of 2×10^6 pores per cm², were cut into small pieces with a diameter of 1 cm. The non-malignant and cancer cells were grown on both sides of the membrane. The selected size of the membrane pores prevented the mixing of non-malignant cells (introduced into the upper part of the microsystem) and cancer cells (introduced into the lower part of the microsystem). At the same time, it was possible to main-



tain contact between non-malignant and cancer cells, create intercellular connections and support their mutual interactions.³⁰ The membrane allowed for constant contact between the co-cultured cells, imitating the physiological conditions of the tumor microenvironment and the ECM. Commercially available membranes were cut with a scalpel from ThinCert inserts (Greiner).

To prepare the designed microsystem, the technique of casting a non-crosslinked mixture of PDMS prepolymer with a crosslinking agent in a weight ratio of 10 : 1 and bonding with oxygen plasma was used. The mold with the geometry was obtained by the photolithography method, based on a capillary film with a thickness of 50 μm (ProCap). The detailed description of these methods can be found in our previous works.^{31,32}

Double-layered cell culture in the microfluidic system

Before starting the cell culture in the microsystem, the device was sterilized. For this purpose, a solution of ethyl alcohol with a concentration of 70% vol. was introduced into the microsystem for 20 min. After sterilization, the microsystem was filled with culture medium, sealed, and incubated overnight (37 °C, 5% CO₂). Then, a suspension of non-malignant cells (keratinocytes or fibroblasts) with a density of 10⁶ cells per ml was prepared, and then it was introduced into the upper part of the chambers in the microsystem with a flow rate of 10 $\mu\text{l min}^{-1}$. Non-malignant cells introduced into the microsystem were incubated for 24 h (37 °C, 5% CO₂). After this time, the cells adhered to the upper surface of the PET membrane (Fig. 1B). Then, the microsystem was rotated 180° to prepare it for the introduction of cancer cells. A suspension of cancer cells with a density of 10⁶ cells per ml was prepared and then analogously introduced to the lower parts of the culture chambers (Fig. 1B). The microsystem was incubated for 24 h (37 °C, 5% CO₂). After this time, the cancer cells adhered to the lower surface of the PET membrane. In this way, a 3D culture was obtained in the form of a double monolayer of non-malignant and cancer cells. During the culture, the medium in the microsystem was changed daily. The cultured cells were monitored with an inverted microscope (Olympus IX71).

Evaluation of cell viability in a microfluidic system

The AlamarBlue assay was used to study the viability and metabolic activity of cells cultured in a microsystem. AlamarBlue test is based on the reduction of non-fluorescent resazurin to fluorescent resorufin by metabolically active cells.³³ A solution of the AlamarBlue reagent (BioRad) with a concentration of 10% vol. was prepared in the DMEM culture medium (Biowest). The solution was loaded into the microsystem (for 15 min, at a flow rate of 2 $\mu\text{l min}^{-1}$). The microsystem with the cells was incubated for 45 min (37 °C, 5% CO₂), and then the fluorescence intensity was measured ($\lambda_{\text{ex}} = 552 \text{ nm}$, $\lambda_{\text{em}} = 582 \text{ nm}$) using a multiwell plate reader (Varian Cary Eclipse Fluorescence Spectrophotometer, Agilent). The measured fluorescence intensity was directly proportional to the number of metabolically active (living) cells in the population. The end

point at which fluorescence intensity was measured (fluorescence maximum) was determined experimentally by monitoring changes in resorufin fluorescence intensity in time (in 5-minute intervals) in culture chambers of the microsystem.

Analysis of cell shape parameters and arrangement of cells on the membrane

The cells cultured in the microsystem were exposed to flow rate and gravity. On each day of the culture, one of the cell types in the microsystem was grown in the direction of gravity. On the second day of the culture, these were non-malignant cells (HaCaT or HMF), while on the third and fourth days – these were cancer cells (MeWo or MCF-7). To evaluate the effect of physical factors (flow rate and gravity) on the adhesion of non-malignant and cancer cells to PET membrane, shape factor, and cell sphericity were determined. Both parameters were determined using CellSens software (Olympus) algorithms. The analyzed cells were stained with CellTracker fluorescent dyes (Invitrogen). Non-malignant cells were stained with CMFDA, showing green fluorescence. Keratinocytes or fibroblasts were incubated with 1 ml of CMFDA dye solution at a concentration of 5 $\mu\text{g ml}^{-1}$ for 45 min (37 °C, 5% CO₂). Cancer cells were stained with CMTPX red dye. For this purpose, the cells were incubated with 1 ml of the CMTPX solution at a concentration of 6.25 $\mu\text{g ml}^{-1}$ for 45 min (37 °C, 5% CO₂). Working solutions were prepared by 1000-fold dilution of stock dye solutions (dissolved in DMSO) in DMEM culture medium without FBS and phenol red.

In order to visualize the cell culture in the microfluidic system, cells cultured on the membrane and stained with cell trackers were imaged using scanning laser confocal microscopy (Zeiss Axio Observer with LSM 900). A Z-axis scan of the cell culture was performed on the first day after introducing the labeled cells into the microsystem.

Evaluation of cytotoxicity and photocytotoxicity of anticancer compounds in the microscale

Staining with propidium iodide and calcein-AM. Differential staining with fluorescent dyes: calcein-AM (CAM), and propidium iodide (PI) of live and dead cells in the population was used to determine cell viability in the microsystems. CAM has the ability to penetrate the biological membranes of living cells. The CAM inside the cell shows green fluorescence when excited with blue light. PI is a compound intercalating between cell DNA. It cannot penetrate intact cell membranes; therefore, it penetrates only into the nuclei of dead cells. PI exhibits red fluorescence when excited with green light. A solution containing: 1 μl of 1 mg ml⁻¹ PI (aqueous solution), 1 μl of 2 mM CAM (DMSO solution), and 500 μl of DMEM culture medium was introduced into the microsystem with cultured cells. The prepared dye solution was introduced into the microsystem at a flow rate of 2 $\mu\text{l min}^{-1}$. The cells were incubated with fluorescent dyes for 10 min (37 °C, 5% CO₂), and they were observed with an inverted fluorescence microscope (Olympus IX71). Cell viability was determined based on the



ratio of viable cells to the total cells in an image from a representative area of the culture chamber. The effect of the tested compounds on the viability of the cell co-culture in the microsystem was assessed (without distinguishing between the viability of non-malignant and cancer cells).

Chemotherapy procedure. Doxorubicin solutions in the concentration range of 0 μM to 100 μM were prepared in a DMEM culture medium without phenol red. 24 hours after formation of the double monolayer of cells in the microsystem, the DOX solutions were introduced into the microsystem for 15 min (flow rate 2 $\mu\text{l min}^{-1}$). The cells in the microsystem were incubated with doxorubicin solutions for 24 h (37 $^{\circ}\text{C}$, 5% CO_2), and then their viability was assessed by differential CAM/PI staining. The control was untreated cells (DOX concentration = 0 μM).

Photodynamic therapy procedure. The photosensitizer (TPP) solutions in the concentration range of 0 μM to 15 μM were prepared in the culture medium DMEM without FBS. The solutions were loaded into the microsystems for 15 min (flow rate 2 $\mu\text{l min}^{-1}$). The cells in microsystems were incubated with photosensitizer solutions for 24 h (37 $^{\circ}\text{C}$, 5% CO_2). First, TPP cytotoxicity was performed using CAM/PI staining. To test the photocytotoxicity of TPP, the cells were additionally irradiated with an LED (10 min, $\lambda = 640 \text{ nm}$, 40 mW cm^{-2}). During irradiation, the cells were 10 mm viability was assessed using the differential CAM/PI staining. The cells untreated with TPP were used as controls in the cytotoxicity study (TPP concentration = 0 μM), while in the photocytotoxicity study, in order to exclude the effect of light on cell viability, irradiated cells without the drug were the control.

Data analysis

The results of all experiments were presented as the mean \pm standard deviations. Error bars report the results of 3 independent experiments (each with three repetitions) or from three independent measurements (in the case of sphericity and cell shape analysis). Using one-way analysis of variance (ANOVA), the Origin Pro 8 software was used to perform statistical analysis. Significant statistical differences are marked with asterisks in the graphs and were determined for the level of significance $\alpha = 0.05$.

Results

Characteristics of the developed models of melanoma and breast cancer

Study of the distribution/arrangement of the double layer of cells in culture chambers on the example of breast cell co-culture. The analysis of microscopic images of breast cells, seeded in the developed microsystem and stained with CellTrackers showed that both cell lines adhered to both surfaces of the PET membrane. It was observed that the cells were arranged regularly in all six chambers of the microsystem. Both, cancer cells (marked in red in Fig. 2A) and non-malignant cells (indicated in green in Fig. 2A) adhered evenly in a

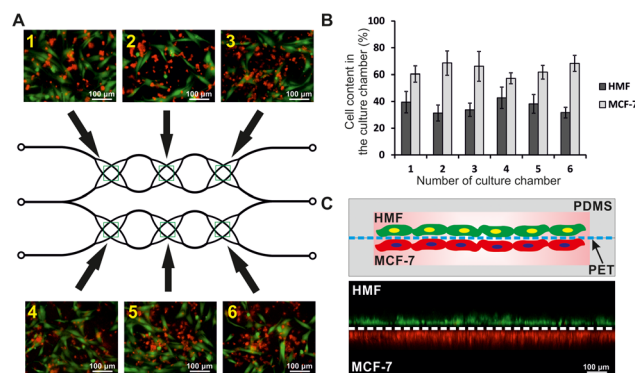


Fig. 2 (A) The regular distribution of non-malignant and cancer cells in double-sided chambers of the developed microsystem. (B) The content of non-malignant and breast cancer cells in the culture chambers of the microsystem – comparison of the seeding density of cells on both sides of the membrane. (C) Z-stacked image of cell culture on a membrane from a confocal microscope. Two layers of cells were adhered to a porous membrane and formed a 3D culture.

common culture part (in a double-sided culture chamber). The distribution of cells in each chamber of the microsystem was similar and reproducible. Based on cell counts, the ratio of fibroblasts to cancer cells in representative areas of each chamber was analyzed and was: 1 : 3 (Fig. 2B). The cells were successfully grown on the top and bottom sides of the membrane, indicating that the proposed cell seeding and culturing method is suitable. 3D fluorescence images of cells in the microsystem confirmed that all types of cells were cultured uniformly over the area of the membrane, forming a double-layered structure (Fig. 2C). The results showed that the developed geometry of the microsystem enabled the culture of a double monolayer of non-malignant and cancer cells (3D model) and its use for modeling cancer disease and drug screening in the following stages of work.

Analysis of cell adhesion to PET membrane based on cell sphericity and shape factor. In the next research stage, it was assumed that the developed microsystem would enable the culture of the cell double-layer for several days. The adhesion of non-malignant and cancer cells to the PET membrane in four consecutive days of culture was assessed. Two shape parameters were analyzed: sphericity and shape factor. The sphericity is a factor defining how much the shape of the analyzed object is similar to a perfect sphere. The values of this factor range from 0 to 1, and low values indicate the ellipsoidal shape of the analyzed object. The sphericity determined in the cellSens software is a function of the diameters of the object. The shape factor determined in the presented research is a parameter characterizing the circularity of the object. The values of this factor also range from 0 to 1. Low values of this factor are characteristic of highly branched objects. The shape factor determined in the cellSens software is a function of the perimeter and surface area of the analyzed object. The values of both analyzed parameters are dimensionless quantities. The obtained values of both tested parameters for all tested cells are shown in Fig. 3. If the value of each parameter was



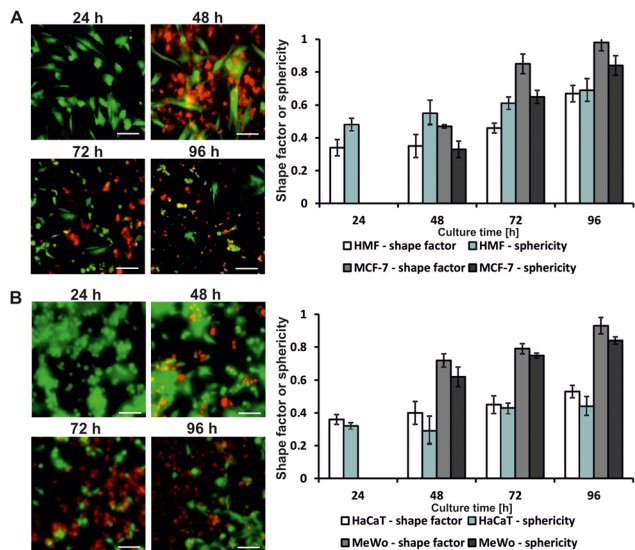


Fig. 3 Comparison of the morphology of the cells cultured in the microsystem on PET membrane and the shape parameters of the cells in the following days of culture (A) for breast cells and (B) for skin cells. Scale bar: 100 μ m.

close to 1, the cells were more spherical, and cell adhesion to the substrate was reduced.

It was confirmed that the force of gravity had little effect on the adhesion of fibroblasts and keratinocytes at the beginning of the culture, but after three days (72 h) of culture, it caused the detachment of cancer cells from the surface of the PET membrane (Fig. 3A and B). An increase in the sphericity and shape factors was observed for each of the cultured cell types. The greatest difference in the values of the measured parameters was noted for MCF-7 cells. Both the shape factor and the sphericity for this cell line increased by 0.51 over the two days of culture. Fig. 3 shows changes in the morphology of non-malignant and cancer cells of the breast and skin cultured on the PET membrane in the following days of culture. It was observed that on the third (72 h) and fourth day (96 h) of culture, the cells were shrunken, and their adhesion to the membrane was lower than on the first (24 h) and second day (48 h) of culture. However, it has been proven that the developed microsystem allows for at least 4-day layered and 3D culture of breast and skin cells.

Analysis of cancer-on-a-chip model viability. Changes in the morphology of cells growing on the membrane did not indicate whether the culture method affected their viability. For this reason, an analysis of cell viability was carried out during the 4-day culture. The influence of the presence of keratinocytes or fibroblasts on the viability of cancer cells (melanoma or breast cancer cells) in cell co-culture was also analyzed.

Studies on optimization of the incubation time of cell co-culture in a microsystem with AlamarBlue reagent showed that the maximum fluorescence intensity is emitted by resorufin in metabolically active cells after 45 minutes of incubation (37 $^{\circ}$ C, 5% CO_2) (Fig. 4A). The measurement in the micro-

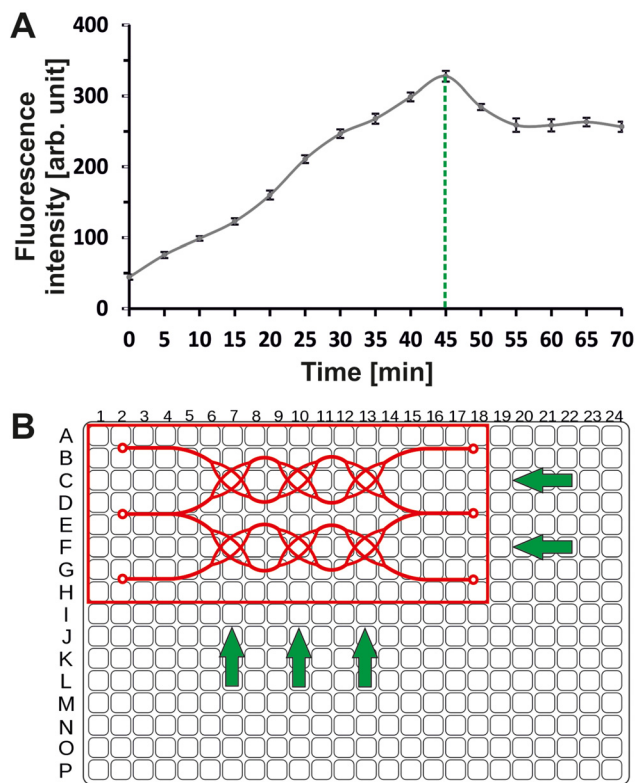


Fig. 4 (A) Optimization of cell incubation time in the microfluidic system with AlamarBlue reagent. The maximum fluorescence intensity of resorufin was noted after 45 min. (B) Matching the layout of the chambers in the microfluidic system to the arrangement of the wells on a standard 384-well plate.

system was possible by matching the arrangement of the culture chambers in the microsystem to the arrangement of the well in a standard 384-well plate (Fig. 4B).

The obtained results showed that cells grown in the layered form increased extensively over the four days of culture. The mean number of cells in the chamber observed on the fourth day increased about 6-fold (compared to the first day of culture) (Fig. 5A) for skin cells co-culture and more than 6-fold for breast cell co-culture. The changes in cell viability and morphology were confirmed by microscopic observations (Fig. 5A and B).

Application of skin and breast cancer models for the screening of anticancer drugs

Photodynamic therapy on a microscale layered melanoma-on-a-chip model. The developed melanoma model was used to evaluate the cyto- and photocytotoxic properties of TPP. It was shown that the tested photosensitizer was non-cytotoxic in the concentration range from 0 μ M to 5 μ M; therefore, such photosensitizer concentrations could be used in the PDT procedure (Fig. 6A). After irradiating of the cells cultured in the microsystem, their viability decreased to: $44.63 \pm 22.57\%$, $50.89 \pm 28.68\%$ and $29.92 \pm 17.94\%$ (of control) for 1 μ M, 3 μ M and 5 μ M of TPP, respectively (Fig. 6A).



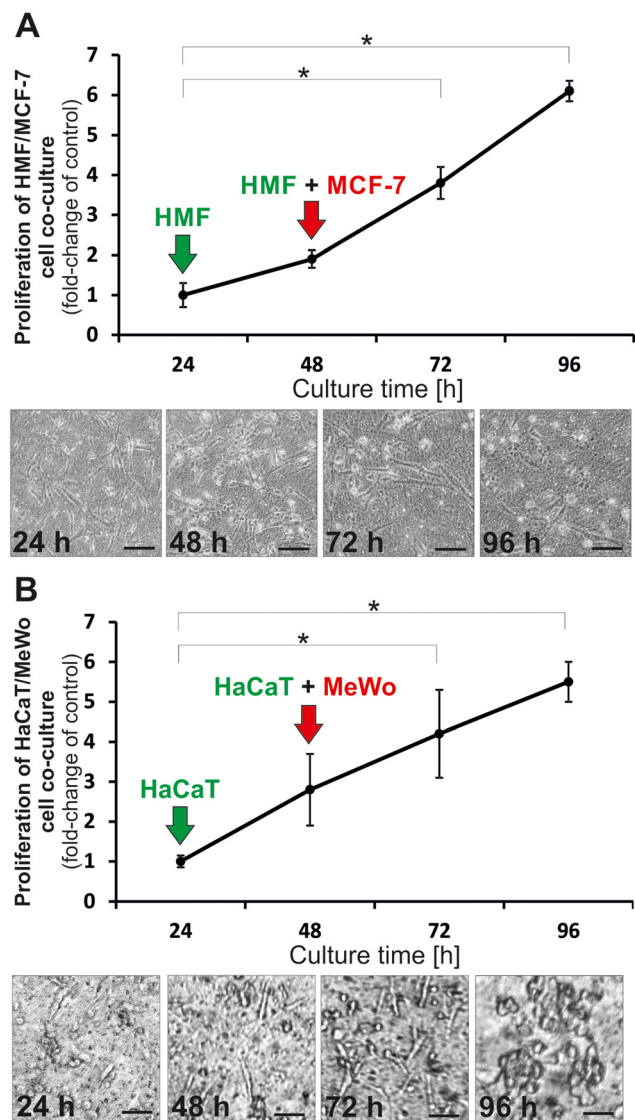


Fig. 5 Viability of (A) breast cell co-culture (HMF/MCF-7) and (B) skin cell co-culture (HaCaT/MeWo) in the microsystem determined by the AlamarBlue test (*ANOVA, $\alpha = 0.05$, $n \geq 3$). Phase-contrast images show cell morphology on a porous PET membrane. Scale bar: 100 μm .

The obtained results were confirmed by fluorescence microscope images with stained cells (PI/CAM) (Fig. 6B). The results proved that TPP meets the requirements for a photosensitizer because it is not cytotoxic in the dark but photocytotoxic on cancer skin cells after light activation. Therefore, the PDT with TPP could be an effective method of melanoma treatment. The developed melanoma-on-a-chip model was suitable for modeling the disease and testing the effectiveness of anticancer therapies.

Cytotoxicity analysis on a layered breast cancer-on-a-chip model. The developed microsystem with 3D layered model of breast cancer was used to study cell viability after a chemotherapy procedure. The cytotoxicity of doxorubicin (DOX) in the range of 0 μM to 100 μM was examined. The analysis of the obtained results showed that the number of viable fibroblasts

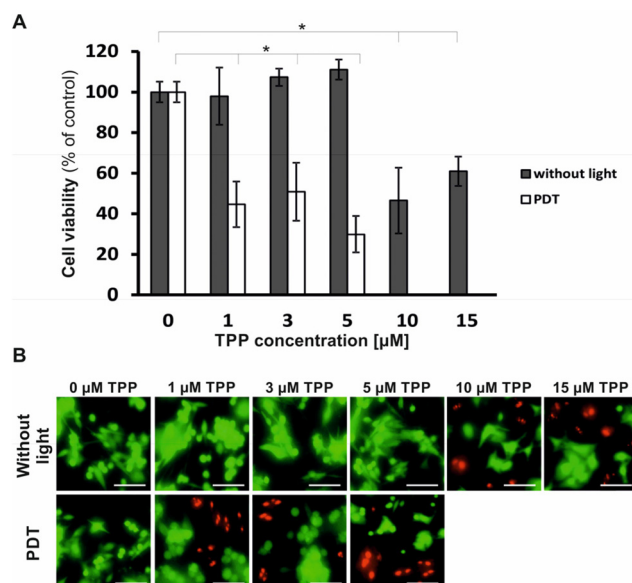


Fig. 6 (A) The results of cell viability before (without light) and after PDT with TPP (*ANOVA, $\alpha = 0.05$, $n \geq 3$). (B) The cells were stained using CAM/PI, scale bar: 100 μm .

and breast cancer cells cultured on the PET membrane scaffold decreased with the increase in the concentration of the tested compound. At the lowest tested concentration of DOX (0.1 μM), breast cell viability was 71.6% \pm 22.4%. However, after incubation with higher concentrations of DOX, cell viability was significantly lower. It equaled 30.7% \pm 2.1% and 23.9% \pm 3.1% for concentrations 10 μM and 100 μM , respectively (Fig. 7A). Because doxorubicin solutions were introduced into the microsystem through microchannels located in the upper PDMS layer, the observed decrease in cell

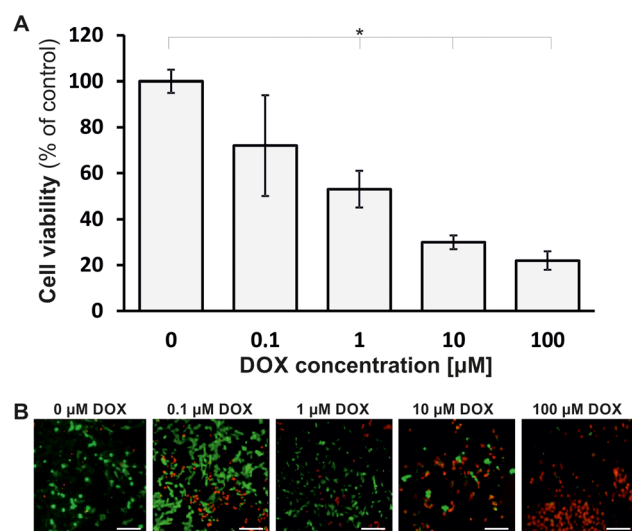


Fig. 7 (A) The cells stained with CAM (green-alive cells) and PI (red – dead cells) (B) cell viability after chemotherapy with DOX (*ANOVA, $\alpha = 0.05$, $n \geq 3$).



viability confirmed that the solutions of the test compound penetrated into the cancer cells through the fibroblast layer and the pores in the PET membrane. This means that the porous PET membrane can be successfully used for 3D cell culture and for testing the permeability of and the layer imitating the cancer stroma. CAM/PI staining for each tested drug concentration is shown in Fig. 7B.

Discussion

The aim of our work was to develop a microfluidic cellular model that would mimic the complex structure of a tumor under *in vitro* conditions. The work assumed that the developed cellular model would be universal and enable the modeling of cancer diseases in a reproducible, representative, and useful way for screening anticancer drugs. It was assumed that the developed double-layer culture of non-malignant and cancer cells on a biocompatible polymer membrane could be successfully used to assess the toxicity of anticancer compounds. Therefore, a new microfluidic system was developed, equipped with a scaffold made of a porous PET membrane. The microsystem was used for layered co-culture of non-malignant (HMF) and cancer (MCF-7) breast cells as well as keratinocytes (HaCaT) and cancer (MeWo) skin cells.

The developed cancer-on-a-chip microsystems allowed the co-culture of stromal cells (fibroblasts or keratinocytes) with cancer cells for several days. All cell types used in the experiments adhered to the porous substrate 24 h after introduction into the microsystem and showed high viability, despite the force of gravity. The use of the PET membrane equipped with pores as scaffolds for non-malignant and cancer cells enabled the interaction between cells to be preserved. The use of the membrane in the construction of the microsystem made it possible to physically separate the two types of cultured cells and simultaneously ensure their mutual contact. The cells in the microsystem were cultured in the form of a spatial, double monolayer. We proved it was possible to perform cell culture for 4 days in the microsystem, during which the viability of the cells was maintained at a high level. The double-layer co-culture of cells on a polymer scaffold allowed for a high surface-area-to-volume ratio (SAV) in the culture.^{34,35} As a result, the conditions in the microsystem allowed to reflect selected aspects of cancer heterogeneity (the stroma made of non-malignant cells) and of the conditions in the cancer microenvironment (microflow).

The developed cell model in the microsystem was used to study the cytotoxicity and photocytotoxicity of anticancer compounds. In the case of photosensitizer studies on a melanoma-on-a-chip cell model, results consistent with results presented in the literature were obtained. Żuchowska *et al.* studied encapsulated *meso*-tetraphenylporphyrin in a spheroidal model of breast cancer in a microfluidic system. As in the case of the layered cell model, the cytotoxic and photocytotoxic effects of TPP were demonstrated, but at higher concentrations of TPP.³⁶ The cytotoxicity of doxorubicin in breast cancer

models has also been studied in the literature. Yildiz-Ozturk *et al.* confirmed the dose-effect relationship in a concentration range similar to tested in our study.³⁷ The literature data clearly confirms that the layered cell model can be successfully used for the screening of cytotoxicity or photocytotoxicity of compounds.

Among the literature reports, one can find examples of microsystems for cell culture with the use of membranes. Choi *et al.*³⁸ developed a microfluidic system to mimic the spatial structure of early-stage breast cancer. Spheroids formed from breast cancer cells (MCF10 DCIS) were co-cultured in a microsystem with human mammary epithelial cells (HMT-3522) and breast fibroblasts (HMF). Cell culture was carried out using protein membranes that acted as extracellular matrix. Similarly, Mondrinos *et al.*³⁹ developed a three-dimensional cell co-culture that mimics the structure of a tumor. Researchers cultured human endothelial cells (HUVEC), bronchial epithelial cells (BEAS-2b), human lung fibroblasts (NHLFs), and lung cancer cells (A549) on semipermeable hydrogel membranes that also mimicked the structure and function of the ECM. In both cases, spheroid cultures were used to replicate *in vitro* interactions between stromal cells and cancer cells. Due to the significant advantage over other 3D models, layered cultures have become the subject of interest of scientists in recent years.^{40,41} Okh *et al.*²⁷ proposed a layered skin model in a microfluidic system based on co-culture with nerve cells, representing part of a complex and functional tissue. However, there is still a lack of microsystems for cell cultures that mimic the multilayered structure of a part of cancer tissue, and the system developed by us may be the answer to this need. Similar solutions are used, but mainly for modeling normal (non-malignant) tissues, *e.g.*, skin,⁴² gut,⁴³ heart,⁴⁴ kidney,⁴⁵ or liver.^{46,47} One example of the use of cell culture on a membrane to mimic a disease state is the work of Wufuer *et al.*⁴⁸ They designed a microfluidic system equipped with PET membranes and used it to mimic inflammation and test anti-inflammatory drugs. However, the microsystem for layered 3D cell culture presented in this paper is one of the few microfluidic devices with commercially available porous PET membranes as scaffolds for co-culture of non-malignant and cancer cells and for the use of this type of culture for simple modeling of cancer tissue.

Further work is needed to improve the presented model of layered cell co-culture on the membrane, *e.g.*, to supplement it with a network of blood vessels characteristic of *in vivo* tumor tissues and to add immune cells to the culture in order to reflect the tumor microenvironment better. However, the cell model presented in this paper has an advantage over other *in vitro* cell models because it is simple and highly reproducible, and more similar to physiological tissue than standard 2D and 3D cultures. Finally, it is worth pointing out that the solution proposed in this paper is an excellent model and a good point for further research related to the use of combined photochemotherapy in the treatment of breast cancer, melanoma, and breast cancer metastases to the skin. It can be an interesting alternative to the popular three-dimensional cellular spheroids.



Conclusions

In this paper, we developed a new microfluidic system for the creation of a layered cellular cancer model with non-cancerous stroma on a PET membrane. The developed model is a more advanced alternative to standard two-dimensional *in vitro* cell models. The developed geometry of the microsystem allowed for cell culture in the form of a double monolayer. This type of culture allows for regular and reproducible arrangement of cells in the culture and the maintenance of intercellular communication. We proved that the cancer-on-a-chip cellular model could be successfully used as a microtool for modeling cancer disease and studying drug screening and diffusion into cancer cells. In this study, we used the cells from two types of cancer tissue and successfully tested the effectiveness of two drugs with different activity profiles and mechanisms of action. Due to the versatile design and the use of porous membranes, the microsystem can be used to test membrane permeability, drug penetration through the membrane, and develop 3D models of other types of cancer or non-malignant tissues. For this reason, in the future, the developed microsystem may be used to personalize cancer treatment.

Author contributions

Magdalena Flont was responsible for conceptualization, data curation, formal analysis, investigation, methodology, validation, visualization, writing – original draft. Artur Dybko was responsible for funding acquisition, conceptualization, project administration, supervision, writing – review & editing. Elżbieta Jastrzębska was responsible for conceptualization, resources, formal analysis, supervision, writing – review & editing.

Conflicts of interest

There are no conflicts to declare.

Acknowledgements

The part of work was financed as part of the project: Initiative of Excellence - Research University BIOTECHMED 2 (Warsaw University of Technology), grant number 1820/2/Z01/POB4/2021. The authors would like to thank the students: M.Sc. Eng. Zuzanna Mackiewicz and M.Sc. Eng. Marta Białek for their participation in implementing the presented biological works.

References

- 1 D. Liu, J. Wang, L. Wu, Y. Huang, Y. Zhang, M. Zhu, Y. Wang, Z. Zhu and C. Yang, *TrAC, Trends Anal. Chem.*, 2020, **122**, 115701.
- 2 A. K. Capulli, K. Tian, N. Mehandru, A. Bukhta, S. F. Choudhury, M. Suchyta and K. K. Parker, *Lab Chip*, 2014, **14**, 3181.
- 3 Y. Kang, P. Datta, S. Shanmughapriya and I. T. Ozbolat, *ACS Appl. Bio Mater.*, 2020, **3**, 5552.
- 4 C. Mattiuzzi and G. Lippi, *J. Epidemiol. Glob. Health.*, 2019, **9**, 217.
- 5 K. E. de Visser and J. A. Joyce, *Cancer Cell*, 2023, **41**, 374.
- 6 H. Yang, Y. Wang, P. Wang, N. Zhang and P. Wang, *Cancer Biol. Med.*, 2022, **19**, 319.
- 7 J. A. Eble and S. Niland, *Clin. Exp. Metastasis*, 2019, **36**, 171–198.
- 8 F. Vahidian, P. H. G. Duijf, E. Safarzadeh, A. Derakhshani, A. Baghbanzadeh and B. Baradaran, *Immunol. Lett.*, 2019, **208**, 19–29.
- 9 A. Sontheimer-Phelps, B. A. Hassell and D. E. Ingber, *Nat. Rev. Cancer*, 2019, **19**, 65–81.
- 10 M. Russo, C. M. Cejas and G. Pitingolo, *Prog. Mol. Biol. Transl. Sci.*, 2022, **187**, 163–204.
- 11 Y. He, B. Huang, E. Rofaani, J. Hu, Y. Liu, G. Pitingolo, L. Wang, J. Shi, C. Aimé and Y. Chen, *Microelectron. Eng.*, 2020, **225**, 111256.
- 12 K. Kretzschmar, *J. Mol. Med.*, 2021, **99**, 501–515.
- 13 M. A. Mirea, S. Eckensperger, M. Hengstschläger and M. Mikula, *Cancers*, 2020, **12**, 2508.
- 14 C. Garbe, U. Keim, S. Gandini, T. Amaral, A. Katalinic, B. Holleczek, P. Martus, L. Flatz, U. Leiter and D. Whiteman, *Eur. J. Cancer*, 2021, **152**, 18.
- 15 J. M. Ayuso, S. Sadangi, M. Lares, S. Rehman, M. Humayun, K. M. Denecke, M. C. Skala, D. J. Beebe and V. Setaluri, *Lab Chip*, 2021, **21**, 1139.
- 16 X. Y. Li, L. C. Tan, L. W. Dong, W. Q. Zhang, X. X. Shen, X. Lu, H. Zheng and Y. G. Lu, *Front. Oncol.*, 2020, **10**, 597.
- 17 T. C. Pham, V. N. Nguyen, Y. Choi, S. Lee and J. Yoon, *Chem. Rev.*, 2021, **121**, 13454.
- 18 A. Hrizat and E. Brachtel, *J. Mol. Pathol.*, 2023, **4**, 1.
- 19 H. Lim, M. Koh, H. Jin, M. Bae, S. Y. Lee, K. M. Kim, J. Jung, H. J. Kim, S. Y. Park, H. S. Kim, W. K. Moon, S. Hwang, N. C. Cho and A. Moon, *J. Cell. Physiol.*, 2021, **236**, 7014.
- 20 A. Marconi, M. Quadri, A. Saltari and C. Pincelli, *Exp. Dermatol.*, 2018, **27**, 578.
- 21 L. L. Bischel, D. J. Beebe and K. E. Sung, *BMC Cancer*, 2015, **15**, 1.
- 22 C. Giverso and L. Preziosi, *Int. J. Non. Linear Mech.*, 2019, **108**, 20–32.
- 23 T. Pasman, D. Grijpma, D. Stamatialis and A. Poot, *J. R. Soc., Interface*, 2018, **15**, 20180351.
- 24 A. Albanese, A. K. Lam, E. A. Sykes, J. V. Rocheleau and W. C. Chan, *Nat. Commun.*, 2013, **4**, 2718.
- 25 D. Przystupski, A. Górska, O. Michel, A. Podwin, P. Śniadek, R. Łapczyński, J. Saczko and J. Kulbacka, *Cancers*, 2021, **13**, 402.
- 26 M. Fane and A. T. Weeraratna, *Nat. Rev. Cancer*, 2020, **20**, 89.



- 27 J. Ahn, K. Ohk, J. Won, D. H. Choi, Y. H. Jung, J. H. Yang, Y. Jun, J. A. Kim, S. Chung and S. H. Lee, *Nat. Commun.*, 2023, **14**, 1488.
- 28 E. Andreopoulou and J. A. Sparano, *Curr. Breast Cancer Rep.*, 2013, **5**, 42.
- 29 A. E. O'Connor, W. M. Gallagher and A. T. Byrne, *Photochem. Photobiol.*, 2009, **85**, 1053.
- 30 F. R. Walter, S. Valkai, A. Kincses, A. Petneházi, T. Czeller, S. Veszelka, P. Ormos, M. A. Deli and A. Dér, *Sens. Actuators, B*, 2016, **222**, 1209.
- 31 E. Jastrzebska, A. Zuchowska, S. Flis, P. Sokolowska, M. Bulka, A. Dybko and Z. Brzozka, *Biomicrofluidics*, 2018, **12**, 044105.
- 32 E. Jastrzebska, M. Bulka, N. Rybicka and K. Zukowski, *Sens. Actuators, B*, 2015, **221**, 1356.
- 33 F. Bonnier, M. E. Keating, T. P. Wrobel, K. Majzner, M. Baranska, A. Garcia-Munoz, A. Blonco and H. J. Byrne, *Toxicol. In Vitro*, 2015, **29**, 124.
- 34 S. Halldorsson, E. Lucumi, R. Gómez-Sjöberg and R. M. Fleming, *Biosens. Bioelectron.*, 2015, **63**, 218.
- 35 E. W. Young and D. J. Beebe, *Chem. Soc. Rev.*, 2010, **39**, 1036.
- 36 A. Zuchowska, K. Marciniak, U. Bazylińska, E. Jastrzebska, K. A. Wilk and Z. Brzozka, *Sens. Actuators, B*, 2018, **275**, 69–77.
- 37 E. Yildiz-Ozturk, S. Gulce-Iz, M. Anil and O. Yesil-Celiktas, *Cytotechnology*, 2017, **69**, 337–347.
- 38 Y. Choi, E. Hyun, J. Seo, C. Blundell, H. C. Kim, E. Lee, S. H. Lee, A. Moon, W. K. Moon and D. Huh, *Lab Chip*, 2015, **15**, 3350.
- 39 M. J. Mondrinos, Y. S. Yi, N. K. Wu, X. Ding and D. Huh, *Lab Chip*, 2017, **17**, 3146.
- 40 G. Salimbeigi, N. E. Vrana, A. M. Ghaemmaghami, P. Y. Huri and G. B. McGuinness, *Mater. Today Bio*, 2022, **15**, 100301.
- 41 T. Pasman, D. Grijpma, D. Stamatialis and A. Poot, *J. R. Soc., Interface*, 2018, **15**, 20180351.
- 42 S. Lee, S. P. Jin, Y. K. Kim, G. Y. Sung, J. H. Chung and J. H. Sung, *Biomed. Microdevices*, 2017, **19**, 1.
- 43 K. Y. Shim, D. Lee, J. Han, N. T. Nguyen, S. Park and J. H. Sung, *Biomed. Microdevices*, 2017, **19**, 37.
- 44 B. M. Maoz, A. Herland, O. Y. Henry, W. D. Leineweber, M. Yadid, J. Doyle, R. Mannix, V. J. Kujala, E. A. FitzGerald, K. K. Parker and D. E. Ingber, *Lab Chip*, 2017, **17**, 2294.
- 45 K. J. Jang, A. P. Mehr, G. A. Hamilton, L. A. McPartlin, S. Chung, K. Y. Suh and D. E. Ingber, *Integr. Biol.*, 2013, **5**, 1119.
- 46 Y. B. Kang, T. R. Sodunke, J. Lamontagne, J. Cirillo, C. Rajiv, M. J. Bouchard and M. Noh, *Biotechnol. Bioeng.*, 2015, **112**, 2571.
- 47 L. Zhu, H. Xia, Z. Wang, E. L. S. Fong, J. Fan, W. H. Tong, Y. P. D. Seah, W. Zhang, Q. Li and H. Yu, *Lab Chip*, 2016, **16**, 3898.
- 48 M. Wufuer, G. Lee, W. Hur, B. Jeon, B. J. Kim, T. H. Choi and S. Lee, *Sci. Rep.*, 2016, **6**, 37471.

